

cy. 1

**ARCHIVE COPY  
DO NOT LOAN**



## **DEGRADATION OF LOW SCATTER MIRRORS BY PARTICLE CONTAMINATION**

**R. P. Young  
ARO, Inc.**

**VON KÁRMÁN GAS DYNAMICS FACILITY  
ARNOLD ENGINEERING DEVELOPMENT CENTER  
AIR FORCE SYSTEMS COMMAND  
ARNOLD AIR FORCE STATION, TENNESSEE 37389**

**January 1975**

**Final Report for Period February 1 — June 30, 1974**

Approved for public release; distribution unlimited.

Property of U. S. Air Force  
AEDC LIBRARY  
F40600-75-C-0001

**Prepared for**

**SPACE AND MISSILE SYSTEMS ORGANIZATION (DYJB)  
P.O. BOX 92960, WORLDWAY POSTAL CENTER  
LOS ANGELES, CALIFORNIA 90009**

AEDC TECHNICAL LIBRARY



5 0720 00033 7578

## NOTICES

When U. S. Government drawings specifications, or other data are used for any purpose other than a definitely related Government procurement operation, the Government thereby incurs no responsibility nor any obligation whatsoever, and the fact that the Government may have formulated, furnished, or in any way supplied the said drawings, specifications, or other data, is not to be regarded by implication or otherwise, or in any manner licensing the holder or any other person or corporation, or conveying any rights or permission to manufacture, use, or sell any patented invention that may in any way be related thereto.

Qualified users may obtain copies of this report from the Defense Documentation Center.

References to named commercial products in this report are not to be considered in any sense as an endorsement of the product by the United States Air Force or the Government.

This report has been reviewed by the Information Office (OI) and is releasable to the National Technical Information Service (NTIS). At NTIS, it will be available to the general public, including foreign nations.

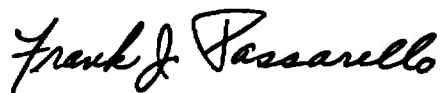
## APPROVAL STATEMENT

This technical report has been reviewed and is approved for publication.

FOR THE COMMANDER



JIMMY W. MULLINS  
Lt Colonel, USAF  
Chief Air Force Test Director, VKF  
Directorate of Test



FRANK J. PASSARELLO  
Colonel, USAF  
Director of Test

# UNCLASSIFIED

REPORT DOCUMENTATION PAGE		READ INSTRUCTIONS BEFORE COMPLETING FORM
1. REPORT NUMBER AEDC-TR-74-109	2. GOVT ACCESSION NO.	3. RECIPIENT'S CATALOG NUMBER
4. TITLE (and Subtitle)  DEGRADATION OF LOW SCATTER MIRRORS BY PARTICLE CONTAMINATION	5. TYPE OF REPORT & PERIOD COVERED Final Report-February 1 to June 30, 1974	
	6. PERFORMING ORG. REPORT NUMBER	
7. AUTHOR(s)  R. P. Young - ARO, Inc.	8. CONTRACT OR GRANT NUMBER(s)	
9. PERFORMING ORGANIZATION NAME AND ADDRESS Arnold Engineering Development Center (DYFS) Arnold Air Force Station Tennessee 37389	10. PROGRAM ELEMENT, PROJECT, TASK AREA & WORK UNIT NUMBERS Program Element 63424F Project 641A	
11. CONTROLLING OFFICE NAME AND ADDRESS SAMSO/DYJB, P. O. Box 92960, Worldway Postal Center, Los Angeles, California 90009	12. REPORT DATE January 1975	
	13. NUMBER OF PAGES 35	
14. MONITORING AGENCY NAME & ADDRESS (if different from Controlling Office)	15. SECURITY CLASS. (of this report)  UNCLASSIFIED	
	15a. DECLASSIFICATION/DOWNGRADING SCHEDULE N/A	
16. DISTRIBUTION STATEMENT (of this Report)  Approved for public release; distribution unlimited.		
17. DISTRIBUTION STATEMENT (of the abstract entered in Block 20, if different from Report)  <i>1. Minors</i>		
18. SUPPLEMENTARY NOTES  Available in DDC.		
19. KEY WORDS (Continue on reverse side if necessary and identify by block number)  optical surface quality mirror surfaces contamination particulate materials		
20. ABSTRACT (Continue on reverse side if necessary and identify by block number)  Mirrors with very low scattering optical surfaces are being used in space borne IR sensors. Dust particles depositing on the surface of these low scatter mirrors can cause an increase in the amount of radiation scattered. A study was made to determine the effect of particle contaminant on the mirror scattering properties. Results of the scattering measurements were compared with predicted values, based on an assumed Lambertian distribution of the scattered radiation. Particles of sizes smaller than the incident radiation		

# UNCLASSIFIED

**UNCLASSIFIED**

20. ABSTRACT (Continued)

wavelength produced less scattered radiation than predicted; whereas, particles of the size or larger than the incident radiation wavelength produced more scattered radiation than predicted.

**UNCLASSIFIED**

## PREFACE

The work reported herein was conducted by the Arnold Engineering Development Center (AEDC), Air Force Systems Command (AFSC), at the request of the Space and Missile Systems Organization (SAMSO), under Program Element 63424F. The results of the tests were obtained by ARO, Inc. (a subsidiary of Sverdrup & Parcel and Associates, Inc.), under ARO Project Number V41P-24B (VC522). Data reduction was completed June 20, 1974, and the manuscript (ARO Control No. ARO-VKF-TR-74-84) was submitted for publication on September 18, 1974.

## CONTENTS

	<u>Page</u>
1.0 INTRODUCTION . . . . .	5
2.0 THEORETICAL MODELS	
2.1 Lambertian Model . . . . .	5
2.2 Flat Mirror Model . . . . .	7
3.0 APPARATUS	
3.1 10.6- $\mu$ m Scatterometer . . . . .	7
3.2 0.6328- $\mu$ m Scatterometer . . . . .	8
3.3 Particle Count Apparatus . . . . .	9
3.4 Near Specular Scatter Photographic Apparatus . . . . .	9
4.0 DATA REDUCTION AND FORMAT . . . . .	9
5.0 PROCEDURE . . . . .	10
6.0 DISCUSSION OF RESULTS	
6.1 Mirror Contaminated in Vertical Position . . . . .	11
6.2 Mirror Contaminated in Horizontal Position . . . . .	13
6.3 Large Particle Contamination . . . . .	14
6.4 Glass Bead Contamination . . . . .	14
7.0 CONCLUDING REMARKS . . . . .	15
REFERENCES . . . . .	15

## ILLUSTRATIONS

Figure

1. 10.6- $\mu$ m Scatterometer	
a. Photograph . . . . .	17
b. Block Diagram . . . . .	18
c. Test Mirror Holder . . . . .	19
2. IR Radiometer . . . . .	20
3. Visible Radiometer . . . . .	21
4. Near Specular Scatter Photographic Apparatus . . . . .	22
5. Mirror with Cover . . . . .	23
6. Particle Count Grid Pattern . . . . .	24
7. BRDF before and after 1176 hr Exposure, Mirror Position Vertical . . . . .	25

<u>Figure</u>	<u>Page</u>
8. Photographs of Near Specular Scattered Radiation before and after 1176-hr Exposure, Mirror in Vertical Position	
a. Clean Mirror . . . . .	26
b. Contaminated Mirror . . . . .	26
9. Photographs of Scattered Radiation at 10 deg from Specular, before and after 1176-hr Exposure, Mirror in Vertical Position	
a. Clean Mirror . . . . .	27
b. Contaminated Mirror . . . . .	27
10. BRDF before and after 45-hr Exposure, Mirror Position Horizontal . . . . .	28
11. Photographs of Near Specular Scattered Radiation before and after 45-hr Exposure, Mirror in Horizontal Position	
a. Clean Mirror . . . . .	29
b. Contaminated Mirror . . . . .	29
12. Photographs of Scattered Radiation at 10 deg from Specular, before and after 45-hr Exposure, Mirror in Horizontal Position	
a. Clean Mirror . . . . .	30
b. Contaminated Mirror . . . . .	30
13. Mirror BRDF with one 750- by 30- $\mu$ m Fiber on Optical Surface . . . . .	31
14. Mirror BRDF with one 90- by 35- $\mu$ m Particle on Optical Surface . . . . .	32
15. Mirror BRDF with Glass Bead (62- to 88- $\mu$ m-diam) Contaminant on Optical Surface . . . . .	33

## TABLES

1. Particle Count in Laser Laboratory Air . . . . .	34
2. Contamination Constants for Mirror Contaminated in Laser Laboratory . . . . .	34
3. Contamination Constants for Mirror Contaminated with Glass Beads . . . . .	34
NOMENCLATURE . . . . .	35

## 1.0 INTRODUCTION

The ability of an IR sensor to detect a low radiance source in the presence of an intense off-axis source is limited, in part, by the energy scattered from the sensor primary mirror. Particulate contamination which can deposit on the mirror surface during sensor fabrication, sensor testing, or during a space mission can increase the amount of scattered energy. For this reason, sensors with good out-of-field rejection requirements are fabricated and tested in modern clean room facilities. However, even in the cleanest of these facilities, it is impossible to prevent some particulate contamination of critical optical surfaces.

An "obscuration factor" can be used as a quantitative definition of the contamination sensitivity of an optical surface such as a mirror. The obscuration factor for particulate contamination is the summation of the projected areas of all the particles resting on the optical surface, divided by the total area of the optical surface. Radiation scattered from particulate contamination has been estimated using the obscuration factor and the assumption of a Lambertian angular distribution of the scattered radiation (Ref. 1). The purpose of this report is to determine the validity of this assumption and to present data obtained after controlled contamination of a high quality, low scatter mirror.

## 2.0 THEORETICAL MODELS

### 2.1 LAMBERTIAN MODEL

The quantity which describes the angular dependence of energy scattered from an optical surface is the bidirectional reflectance distribution function (BRDF). It is defined as the spatial distribution of the ratio of scattered energy to incident energy that is observed by a detector of small angular subtense, normalized to one steradian, taking into account the projected surface area viewed. For near normal incidence of the incident and specular beam, the BRDF can be expressed as

$$\text{BRDF} = \frac{P_s}{P_i \Omega \cos \theta} \quad (1)$$



Measurements were made at angles from the specular beam of less than 14 deg ( $\cos \theta > 0.97$ ); therefore, the BRDF equation can be simplified to

$$\text{BRDF} = \frac{P_s}{P_i \Omega} \quad (2)$$

The scattered energy ( $P_s$ ) is the sum of the energy scattered from the mirror surface and from particles on the surface. Equation (2) can then be expressed as

$$\text{BRDF} = \frac{P_m + P_p}{P_i \Omega} \quad (3)$$

or

$$\text{BRDF} = \frac{P_m}{P_i \Omega} + \frac{P_p}{P_i \Omega} \quad (4)$$

The first term in Eq. (4) is the clean mirror BRDF, and the second term is the BRDF resulting from particles on the mirror surface. At this point, it is assumed that: (1) the particles reflect with a Lambertian angular distribution, (2) the particles are evenly distributed across the mirror surface, and (3) the particles have a reflectivity of one. The irradiance at the mirror surface is the incident energy divided by the area on the mirror illuminated. Therefore, the energy collected by a detector viewing the mirror surface out of the specular reflected beam would be

$$P_p = \frac{P_i}{A_i} \left( \frac{A_p}{\pi} \right) \Omega \quad (5)$$

Substituting Eq. (5) into Eq. (4) gives

$$\text{BRDF} = \text{BRDF}_m + \frac{1}{\pi} \frac{A_p}{A_i} \quad (6)$$

The term  $A_p/A_i$  is defined as the "obscuration factor" for the particles on the mirror surface. For particles which reflect with a Lambertian angular distribution, the increase in mirror scatter due to particulate contamination can be calculated by dividing the obscuration factor by  $\pi$ .

## 2.2 FLAT MIRROR MODEL

Another reflectance model is a flat mirror which would reflect all the incident energy back toward a detector. For this flat mirror model, energy from a particle would be collected only at a discrete angular position, neglecting diffraction. Total mirror BRDF ( $\text{BRDF}_m + \text{BRDF}_p$ ) is as given by Eq. (4). The energy collected by a detector viewing the particle on the mirror surface (assuming the detector much larger than the particle) and out of the specular reflection from the mirror would be

$$P_p = \frac{P_i A_p}{A_i} \quad (7)$$

Substituting Eq. (7) into Eq. (4) gives

$$\text{BRDF} = \text{BRDF}_m + \frac{A_p}{A_i \Omega} \quad (8)$$

The  $A_p/A_i$  term is the obscuration factor. The detector size was assumed larger than the beam reflected from the smaller particle. Therefore, the energy impinging on the detector is not a function of the solid angle subtended by the detector. However, by definition, the BRDF is normalized to a one-steradian field of view. By assuming a detector with a  $10^{-3}$  sr field of view

$$\text{BRDF} = \text{BRDF}_m + 10^3 \frac{A_p}{A_i} \quad (9)$$

By using the flat mirror particle model, Eq. (9) predicts a much higher BRDF increase for a contaminated mirror than was predicted by the Lambertian model. This model probably represents the most severe BRDF degradation which can result from particle contamination on a mirror surface.

## 3.0 APPARATUS

### 3.1 10.6- $\mu\text{m}$ SCATTEROMETER

The 10.6- $\mu\text{m}$  scatterometer is presented in Fig. 1. The system consists of a 3-watt  $\text{CO}_2$  laser, 16-Hz chopper, beam attenuator,

1.25-cm-diam aperture, collection telescope with detector and an angular position readout. The laser operates single mode (TEM<sub>00</sub>) and is polarized in the vertical plane. Beam power distribution is Gaussian, and the effective beam diameter at the test mirror is nominally one cm (1/e power points). Beam attenuation ( $T = 2.2 \times 10^{-5}$ ) is needed when on-axis measurements are made. A helium-neon (He Ne) laser (Fig. 1) beam is aligned paraxial to the CO<sub>2</sub> laser beam after reflection from the germanium window. This permits visual location of the IR beam for system alignment.

The 1.25-cm-diam aperture is mounted at a distance from the test mirror such that its image is formed at the telescope lens. Energy scattered by optical elements up-stream of this aperture and striking the test mirror is focused through the aperture image.

Scattered energy from the test mirror is measured with an IR radiometer (Fig. 2). The radiometer consists of a 6.4-cm focal length germanium lens, telescope barrel, and a 1-mm square pyro-electric detector. The lens is focused so that the detector is imaged at the mirror surface. A field stop is placed in front of the lens limiting the collection optics field of view to 28 by 19 mrad. The radiometer is mounted on a motor driven, two axis gimbal, which is mounted on an arm which pivots about the front surface of the test mirror. Angular arm position is measured with a resolver and digital angle readout. Detector voltage is measured with a lock-in amplifier.

The test mirror used in the contamination study was 5 cm in diameter with a 64-cm focal length. The surface was electroless nickel, deposited on an aluminum blank. The nickel was polished to obtain a very low scatter surface.

### 3.2 0.6328- $\mu$ m SCATTEROMETER

The 0.6328- $\mu$ m scatterometer is essentially the same as the 10.6- $\mu$ m scatterometer as shown in Fig. 1. The alignment He Ne laser is installed in place of the attenuator box and the germanium plate removed. A 250-mm focal length lens is added into the optical path to expand the He Ne beam to approximately 2-cm diameter at the test mirror. The lens replaces the germanium plate and is located at one focal length from the aperture. Since the laser beam is focused at this point, a smaller aperture (0.25-cm-diam) is used.

The IR radiometer is replaced with a 0.6328- $\mu\text{m}$  radiometer (Fig. 3). It consists of a glass lens (5-cm-diam, 100-mm focal length) and a silicon detector (5-mm square). A 5- by 2.5-cm field stop is placed in front of the lens to limit the field of view to 32 by 64 mrad. A current mode preamplifier and lock-in amplifier is used to measure the cell current.

### 3.3 PARTICLE COUNT APPARATUS

Particle count measurement of contamination is made with a 100X binocular microscope. A 100 division reticle is used in the eyepiece. Spacing between divisions is 12.5  $\mu\text{m}$ , as referenced to the microscope stage. Sample movement is provided by a two-axis, linearly translatable stage. Particles on the test mirror surface are illuminated with a standard high-intensity microscope lamp.

### 3.4 NEAR SPECULAR SCATTER PHOTOGRAPHIC APPARATUS

Test apparatus to visibly inspect and photographically record the near angle scatter from the surface of low scatter mirrors is shown in Fig. 4. The system consisted of a point light source, field stop, lens (100-mm focal length), and corner reflector. The point source is imaged on the corner reflector and expanded to fill the test mirror. Light from the test mirror is then focused back to the corner reflector. A camera (not shown in Fig. 4) is placed just behind the corner reflector. Scattered energy in a  $2.4 \times 10^{-4}$  sr cone around the specular reflected beam is recorded on the film plate. Visual inspection is made by looking at the mirror from behind the corner reflector.

## 4.0 DATA REDUCTION AND FORMAT

Mirror BRDF was previously defined as the spatial distribution of the ratio of scattered energy to incident energy that is observed by a detector of small angular sub-tense, then normalized to one steradian (Eq. (7)). The power in the incident beam was many orders of magnitude greater than the power in the scattered radiation; therefore, attenuators had to be used to measure the incident power. To avoid the problem of having to calibrate the attenuators, a diffuse scatterer was used. The mirror BRDF is then expressed as

$$\text{BRDF} = \left( \frac{R_D}{\pi} \right) \left( \frac{V_S}{V_D} \right) \quad (10)$$

The BRDF of the test sample was calculated from the measured detector signal when viewing a diffuse sample and from measurements made from the test mirror.

Scatter data (BRDF) was plotted as a function of angle from the specular beam on semilog paper. An analytical expression which fits the clean mirror data was determined. For the mirror used in these tests, the clean mirror BRDF equation was

$$\text{BRDF}_m = 2 \times 10^{-5} \theta^{-1.5} \quad (11)$$

The measured BRDF of most contaminated mirrors plotted as straight lines on the semilog plots (after the clean mirror contribution was subtracted). An analytical expression for the particulate contribution can be expressed as

$$\text{BRDF}_p = C_1 \frac{A_p}{A_i} e^{-C_2 \theta} \quad (12)$$

The area ratio was the obscuration factor and depended on the amount of contamination on the mirror surface. The constants  $C_1$  and  $C_2$  were calculated from the best straight line curve fit through the experimental data. For a Lambertian distribution of the scattered energy,  $C_1$  would be  $1/\pi$ , and  $C_2$  would be zero. The complete expression for the mirror BRDF was expressed as

$$\text{BRDF} = 2 \times 10^{-5} \theta^{-1.5} + C_1 \frac{A_p}{A_i} e^{-C_2 \theta} \quad (13)$$

## 5.0 PROCEDURE

The mirror contamination test involved contaminating a low scatter mirror, making a particle count to determine the number and size distribution of the particles on the mirror surface, then measuring the BRDF of the contaminated mirror. Mirrors were contaminated by: (1) exposing the mirror in a laboratory environment with the mirror mounted vertically, (2) exposing the mirror in the same environment with the mirror mounted horizontally, face up, and (3) dropping glass beads on the mirror. During exposure, the mirror surface, except for the central 1.3-cm diameter, was covered (Fig. 5). The cover was to prevent large particles from depositing outside the area to be illuminated during BRDF measurements.

After a mirror was exposed to the contaminating environment, the mirror was moved to a class 100, laminar flow clean bench for a particle count (Ref. 2). All particles on the mirror which fell within the grid pattern of Fig. 6 were counted and sized by groups. Size groups used were 5 to 15  $\mu\text{m}$ , 15 to 30  $\mu\text{m}$ , 30 to 75  $\mu\text{m}$ , and particles larger than 75  $\mu\text{m}$ . Particles were sized by maximum diameter or length. Area of the particles in each size group was calculated based on the number of particles in that group, assuming all had a circular projected area of the mean diameter of the group (e.g. 10- $\mu\text{m}$  diameter for the 5 to 15- $\mu\text{m}$  group). The obscuration factor was then calculated by dividing the particle area by the area of the grid pattern.

The next step was to measure the mirror surface BRDF. The diffuse reflector was mounted in the laser beam, and the output from the radiometer was recorded. Next, the test mirror was installed in place of the diffuse reflector. The radiometer was centered on the specular reflection to establish the angular reference. The radiometer was then rotated about the surface of the test mirror in angular steps, recording the detector output at each angle. After the BRDF measurements, scatter photographs were made of the mirror surface.

## 6.0 DISCUSSION OF RESULTS

### 6.1 MIRROR CONTAMINATED IN VERTICAL POSITION

The first method of contaminating the test mirror was to mount the mirror in the vertical position and expose its surface to the air in the laser laboratory (see Table 1 for air particle count). Scatter measurements were made to obtain the mirror BRDF at various angles from specular. Contamination constants  $C_1$  and  $C_2$  (Eq. (13)) were calculated from the measured BRDF and particle count data.

Results of some early IR scatter measurements (Run Nos. 32, 34, 36, and 38) are presented in Table 2. The mirror cover was not used for these runs, and the data may be influenced by large particles out of the central area of the mirror. This may be the reason for the high value for the constant  $C_1$ , calculated after Run No. 34. Average values for constants  $C_1$  and  $C_2$  for these four measurements were 6.9 and 0.096, respectively.

The test mirror was then exposed for 1176 hr in the laser laboratory (vertical position) using the mirror cover. (The cover exposed a 1.3-cm-diam area in the center of the optical surface.) Particle count of the laboratory air is presented in Table 1. Scatter measurements were made with the 10.6- $\mu\text{m}$  scatterometer after 168, 336, 504, 864, and 1176 hr of exposure. Only the results taken after 1176 hr of exposure are presented (Fig. 7) because no increase in IR scatter was observed during this series of tests. Visible (0.6328- $\mu\text{m}$ ) scatter measurements were made only after the mirror was exposed for 1176 hr. At one degree from specular, the BRDF measured at 0.6328  $\mu\text{m}$  for the clean and contaminated mirror were of approximate equal value. However, as the angle from specular increased, so did the separation in the BRDF values.

Some difficulty was experienced in trying to determine the obscuration factor based on a particle count of the mirror surface. No particles of a size greater than 15  $\mu\text{m}$  and only 19 particles in the 5- to 15- $\mu\text{m}$  size range were observed. However, the mirror surface was covered with particles in a size range from 0.25  $\mu\text{m}$  (believed to be the smallest size to be seen visually) to 1  $\mu\text{m}$ , and the area of these particles would have to be included when calculating the obscuration factor. An attempt was, therefore, made to count the particles using a random sample technique. The particle area was calculated assuming a circular area and a 0.625- $\mu\text{m}$  mean particle diameter. The calculated obscuration factor for the very small particles and the 19 other particles was  $6.9 \times 10^{-5}$ . With this value for the obscuration factor, the predicted increase in BRDF for the Lambertian model was calculated to be  $2.2 \times 10^{-5}$ . No increase in BRDF was observed for the IR measurements; however, a larger value than calculated was measured with the 0.6328- $\mu\text{m}$  scatterometer. The contamination constants  $C_1$  and  $C_2$  (Eq. (13)), calculated from the visible scatterometer data, were 8.4 and 0.08, respectively. Constant  $C_1$  was 26 times greater than the value calculated using the Lambertian model (Eq. (6)).

Photographs were taken of the near specular scattered radiation from mirror surface using the apparatus shown in Fig. 4. Photographs of the clean and contaminated mirror are shown in Fig. 8. There is virtually no difference between the clean and dirty mirror photographs, thus indicating no difference in BRDF for angles up to 1 deg from specular (visible radiation). Photographs were also taken with the camera nominally 10 deg from the specular reflection (Fig. 9). A microscope illuminator was used as the light source. The population density of the small particles is apparent from the photograph of the dirty mirror.

Considerably more light was scattered from the contaminated mirror surface (Fig. 9), which is in agreement with the 0.6328- $\mu\text{m}$  scatterometer measurements.

## 6.2 MIRROR CONTAMINATED IN HORIZONTAL POSITION

Scatter measurements were made after exposing the mirror in the laboratory environment (Particle Count in Table 1) with the mirror positioned with its mirrored surface upward (horizontal position). The mirror surface BRDF was degraded during the first two hours of exposure. Results of the IR tests are presented in Table 2 (Run Nos. 72 to 81). The contamination BRDF constant  $C_1$  (Eq. (13)) varied from a low of 1.7 to a high of 7.4. Average value of  $C_1$  for 10 scatter measurements was 3.6, approximately 11 times the value predicted by the Lambertian model (Eq. (6)). The constant  $C_2$  varied from a low of 0.085 to a high of 0.2. Average value for this constant was 0.14.

Angular dependence of BRDF after 45-hr exposure is presented in Fig. 10. The IR contaminated mirror data shows the almost straight line angular dependence of BRDF as plotted on semilog graph paper. The BRDF at 1 deg was nominally 2 orders of magnitude higher for the contaminated mirror than for the BRDF of the clean mirror at the same angle. The separation between the clean and dirty mirror BRDF (IR) increased as the angle from specular increased. The BRDF curve, measured at 0.6328  $\mu\text{m}$ , is lower than the corresponding curve measured in the IR because the 0.6328- $\mu\text{m}$  beam was larger. The contamination density was higher in the center (1.3-cm-diam) than it was at larger diameters; therefore, the effective obscuration factor was lower for the visible scatter measurement. The constants  $C_1$  and  $C_2$  for the visible measurement were 1.62 and 0.17, respectively, with no correction made to the obscuration factor to account for the variation in particle density. The constant  $C_1$  would be larger if such a correction was made.

Figure 11 is a photograph of the near specular scatter for the clean mirror and for the mirror after it was exposed for 45 hr in the laboratory (horizontal position). Particles are visible on the mirror surface, indicating a larger BRDF at 1 deg from specular for the contaminated mirror. A larger BRDF was measured at 1 deg using the 0.6328- $\mu\text{m}$  scatterometer.



Photographs were also taken with the camera nominally 10 deg from the specular reflection. A microscope illuminator was used as the light source. Comparison of the clean and dirty mirror photographs (Fig. 12) illustrates the measured differences in BRDF measured at large angles from the specular reflection. Also seen is the variation of the particle density at different radial distances from the center of the mirror.

### 6.3 LARGE PARTICLE CONTAMINATION

Effects of large particulate contamination on measured BRDF at  $10.6\text{ }\mu\text{m}$  are presented in Figs. 13 and 14. The measured BRDF curves did not approach straight lines; therefore, the constants  $C_1$  and  $C_2$  were not calculated. Calculated BRDF for the contaminated mirrors based on the Lambertian model and the contamination constants (average)  $C_1$  and  $C_2$ , as determined in the previous sections, are also presented in the figures. The measured BRDF at 1 deg for both Run Nos. 12 and 25 was nominally 3.5 times higher than predicted by the empirical model, and roughly 20 times higher than predicted by the Lambertian model.

### 6.4 GLASS BEAD CONTAMINATION

Glass beads (62- to  $88\text{-}\mu\text{m}$ -diam) were used to artificially contaminate the mirror surface. Results of IR scatter tests are presented in Fig. 15 and Table 3. The contaminated BRDF did not plot as a straight line in Fig. 15; however, if a straight line as shown in the figure was used to calculate the constants  $C_1$  and  $C_2$ , a conservative estimate of mirror BRDF would result from calculations using the empirical expression.

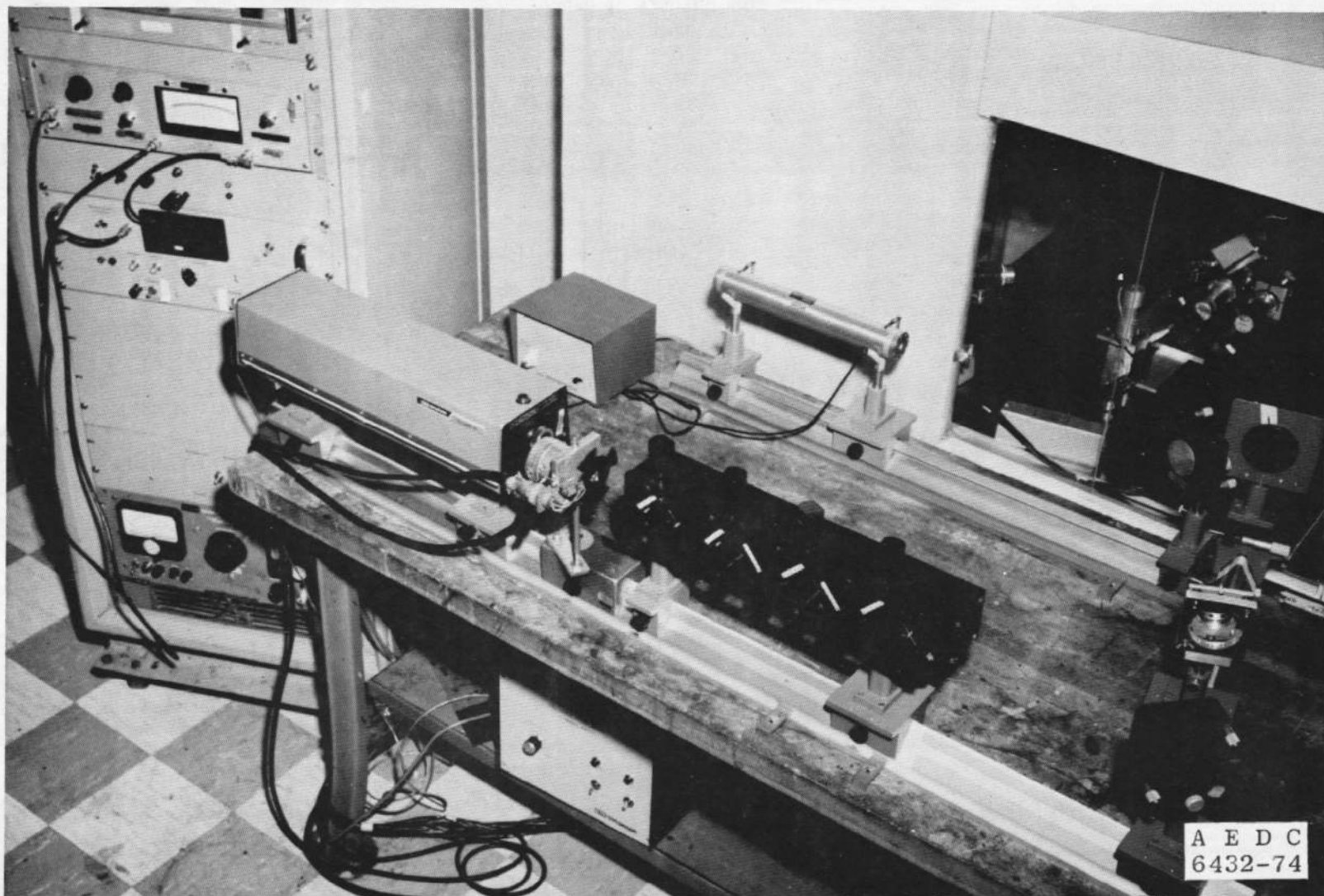
It should be noted in Table 3 that the constant  $C_1$  is very high; nominally 380 times the Lambertian prediction. Also, the constant  $C_2$  has a fairly large value, indicating strong dependence of BRDF on the angle from specular. No BRDF measurements using the glass beads were made with the  $0.6328\text{-}\mu\text{m}$  scatterometer.

## 7.0 CONCLUDING REMARKS

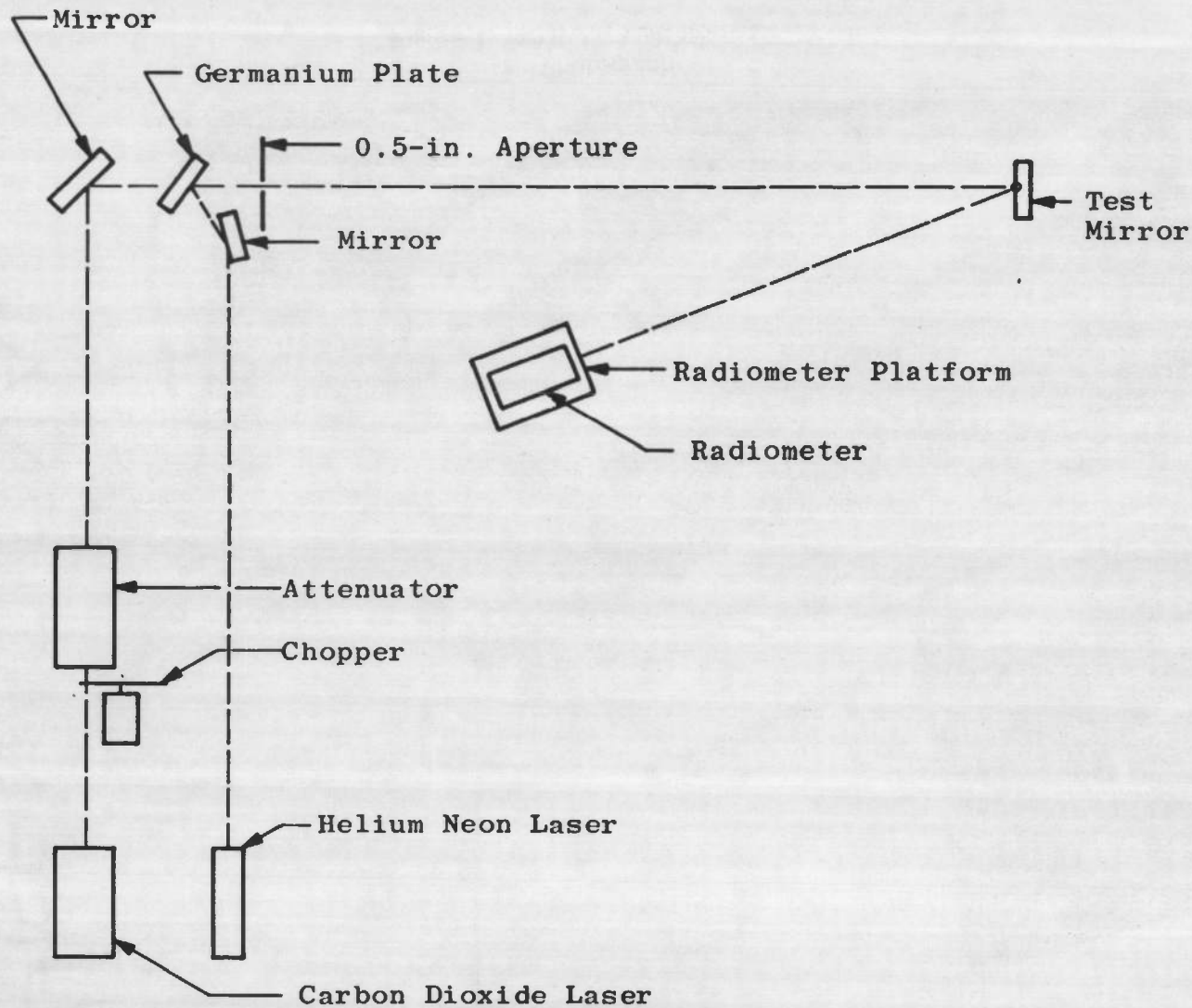
The effect of particle contamination on mirror scatter was investigated. Particles deposited on a mirror surface which are smaller than the incident radiation wavelength produced less scattered energy than was predicted by assuming a Lambertian distribution of the scattered radiation. For particles the size of the radiation wavelength and larger, the scattered energy was greater than predicted by the Lambertian assumption. An empirical expression was presented for predicting the scatter angular dependence for these particles. Contamination constants used in this equation were found to depend on the size and type of contamination deposited on the mirror. As expected, none of the particles deposited on the mirror surface produced scattered radiation of the magnitude predicted by the flat mirror scattering model.

## REFERENCES

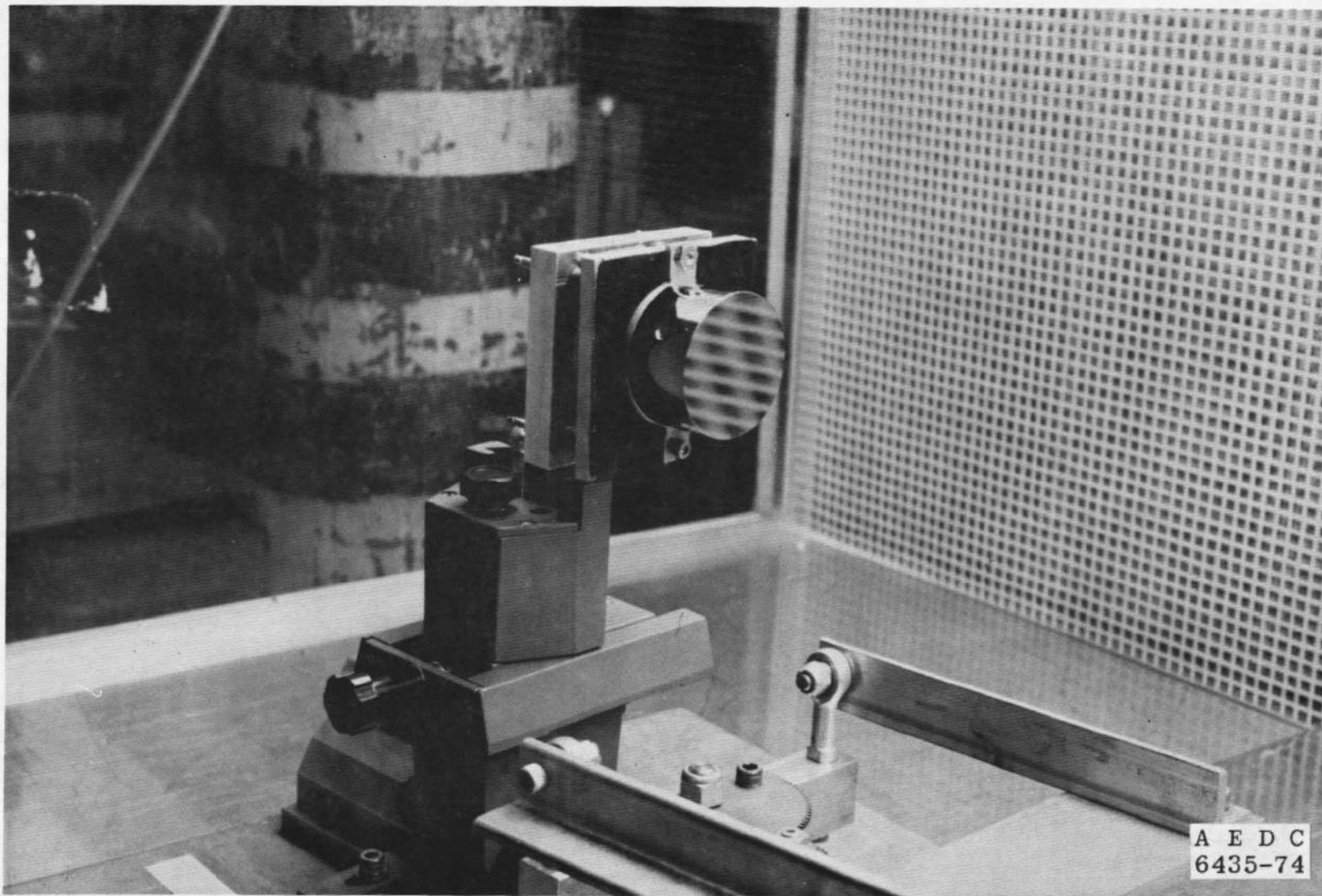
1. Smith, D. C. "Cleanliness Requirements for Space Borne Optical Sensors." AIAA Paper No. 71-471, presented at the AIAA 6th Thermophysics Conference at Tullahoma, Tennessee, April 26 to 28, 1971.
2. "Standard Method for Measuring and Counting Particulate Contamination on Surfaces." STM Designation F24-65, Reapproved 1970.



a. Photograph  
Figure 1. 10.6-μm scatterometer.



b. Block diagram  
Figure 1. Continued.



c. Test mirror holder  
Figure 1. Concluded.



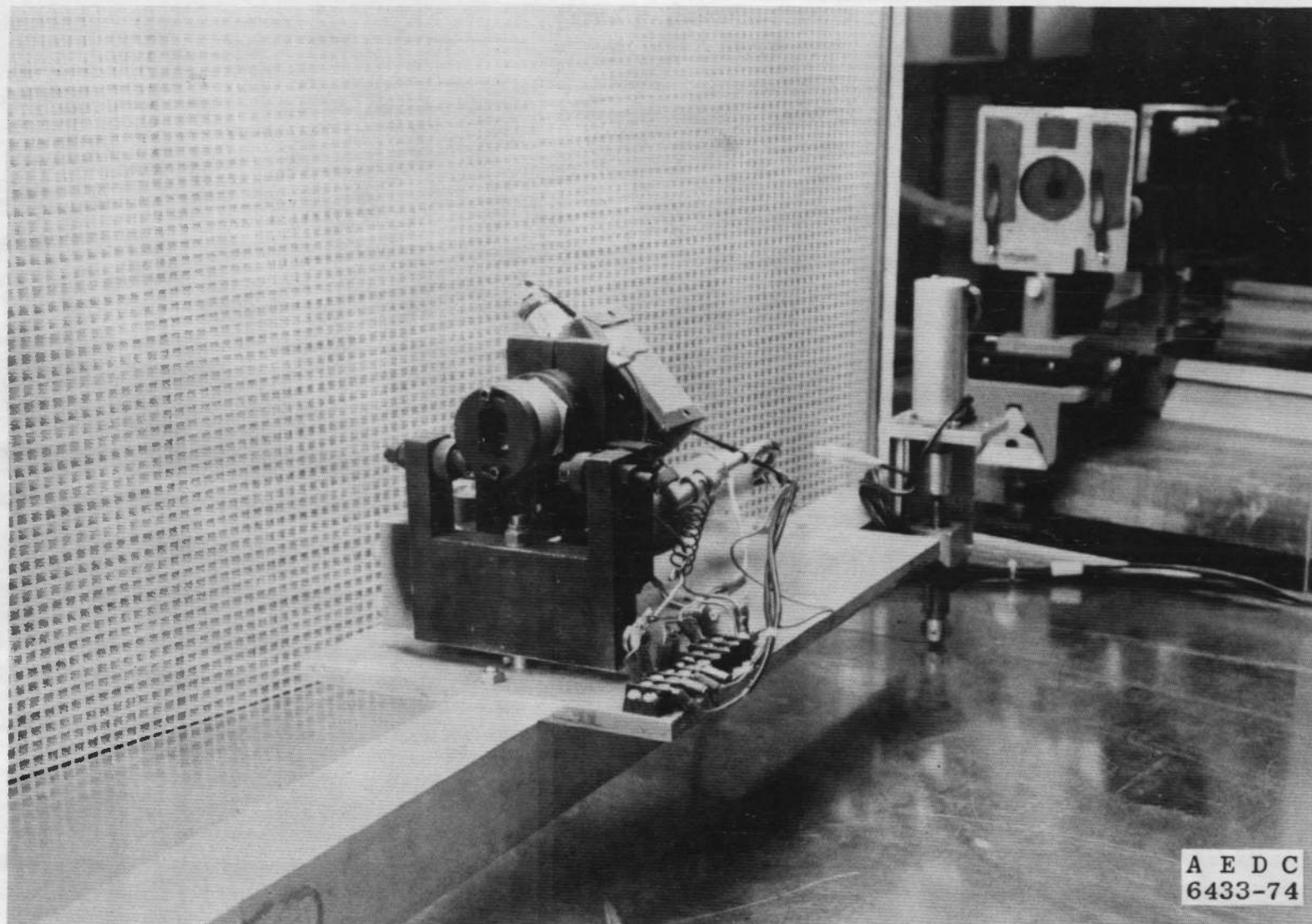


Figure 2. IR radiometer.

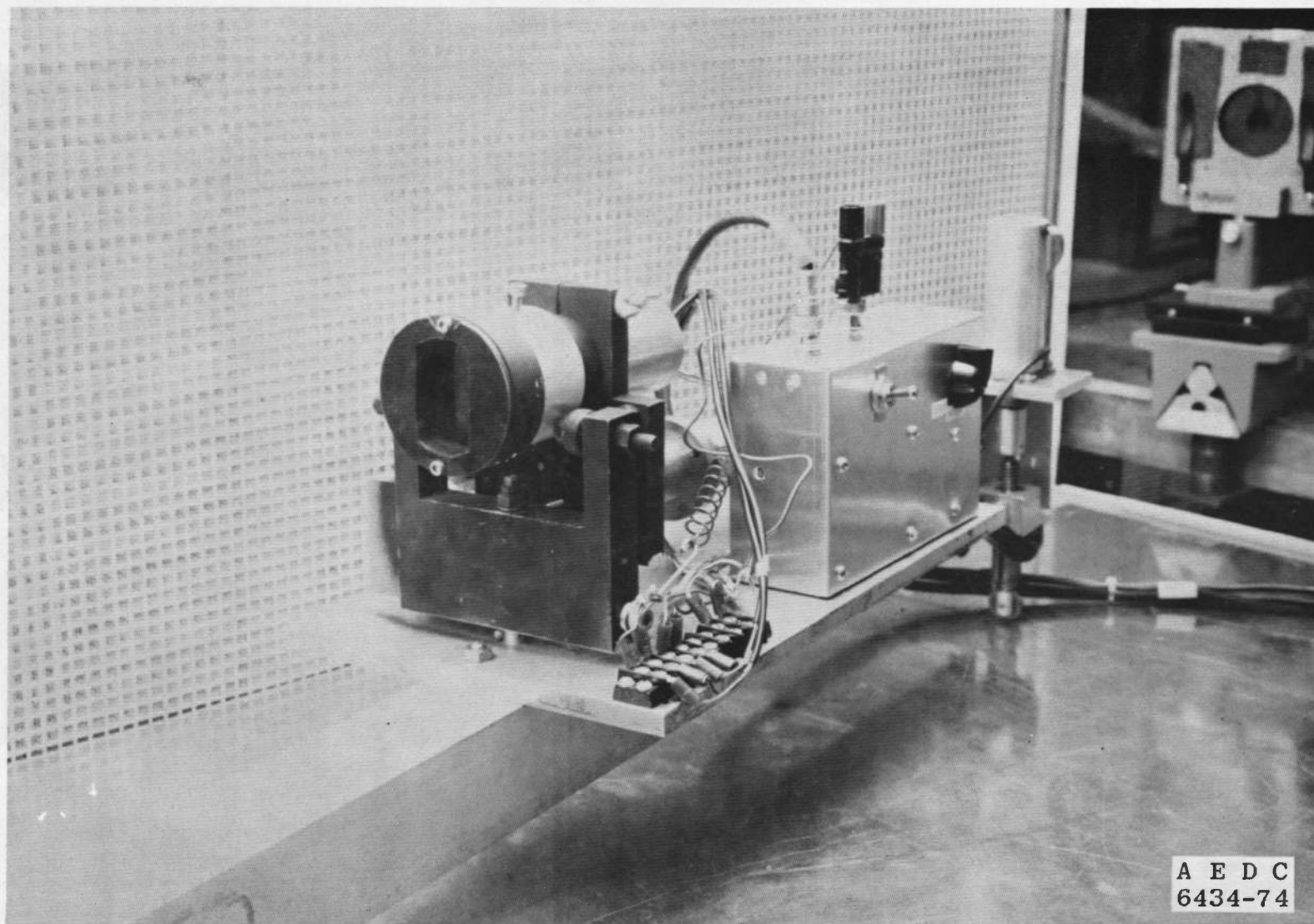


Figure 3. Visible radiometer.

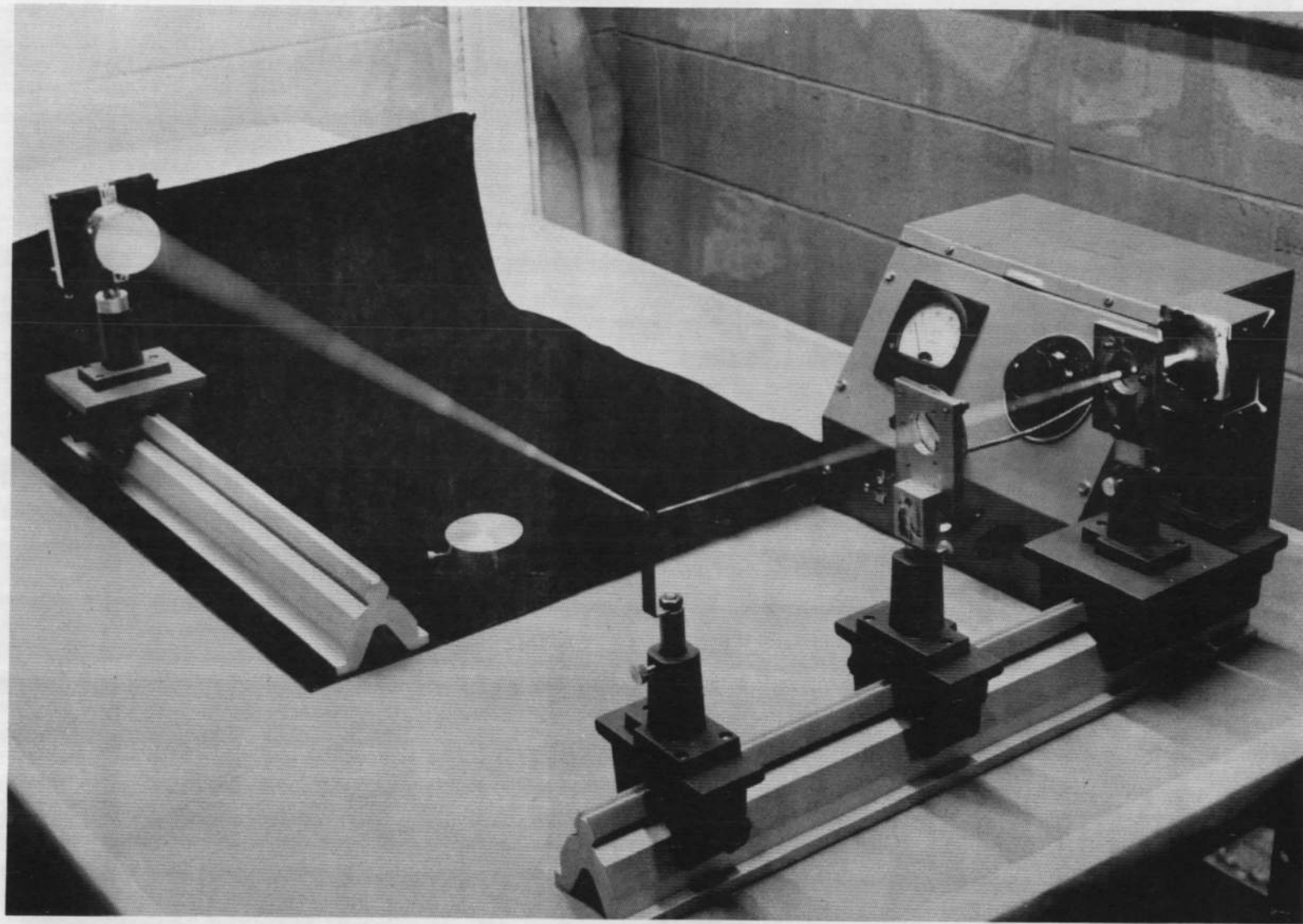


Figure 4. Near specular scatter photographic apparatus.



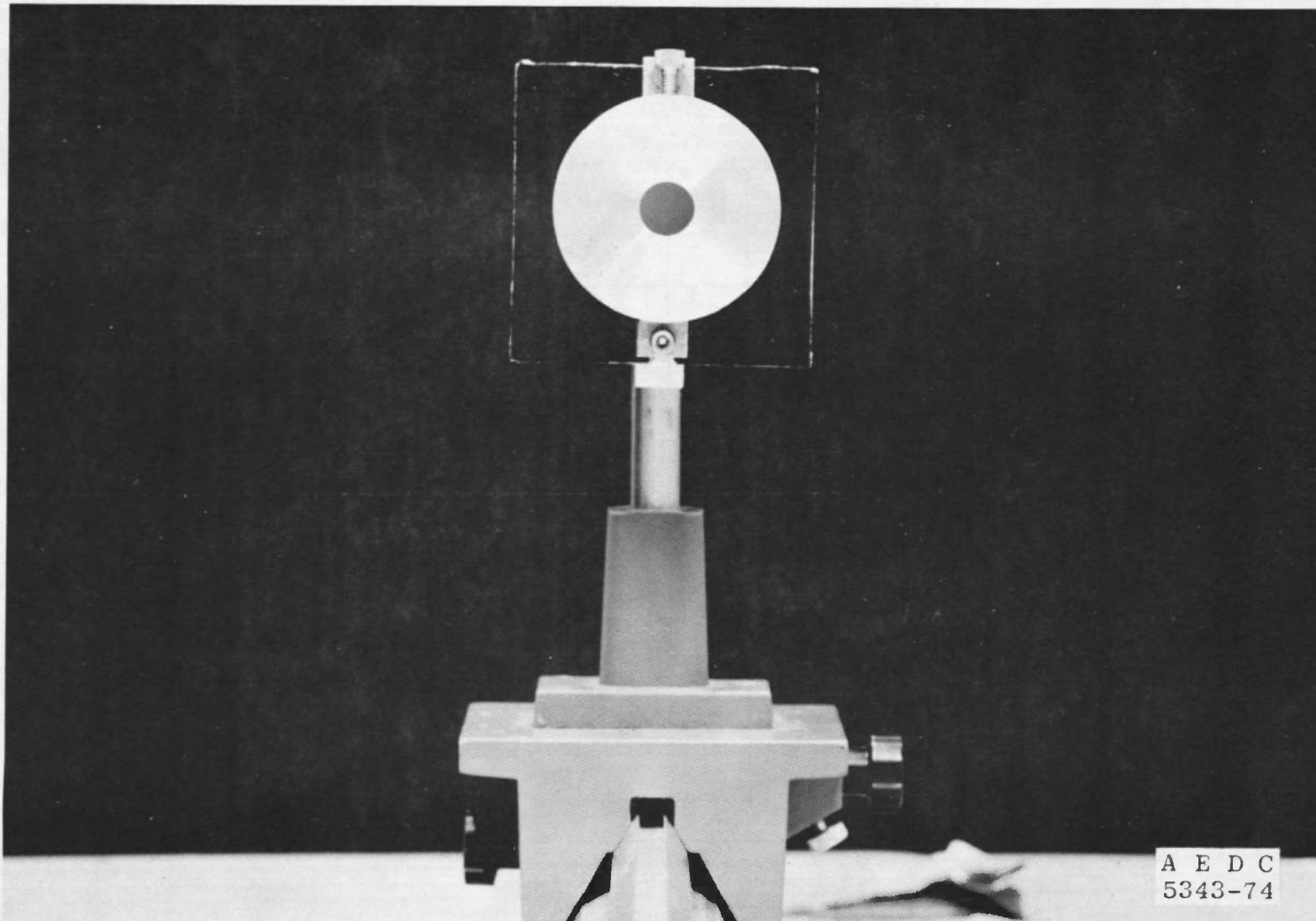
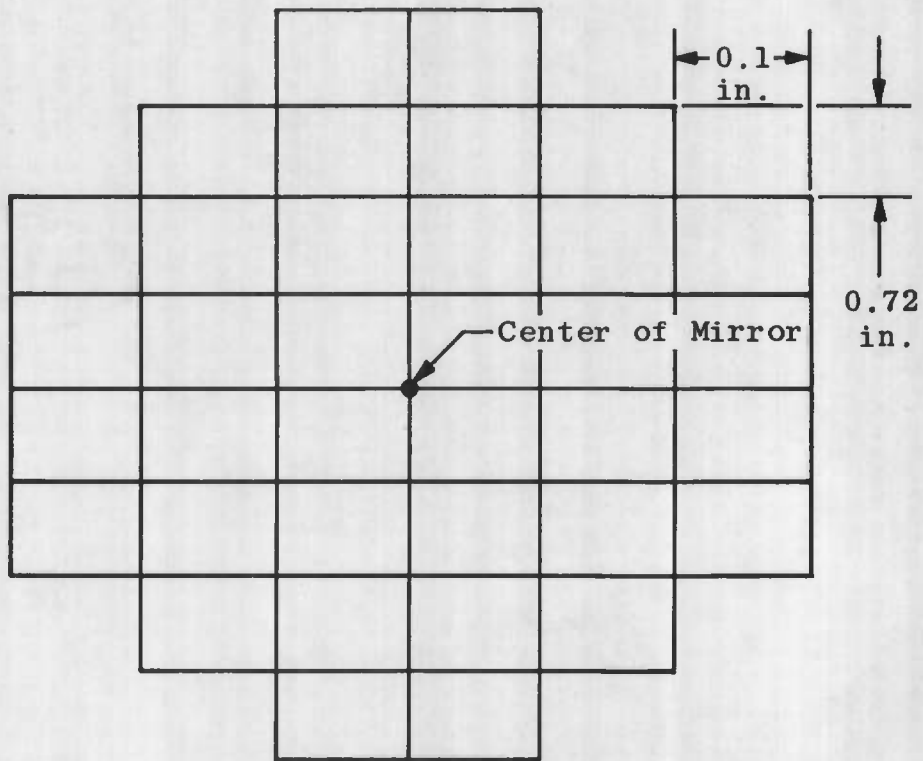


Figure 5. Mirror with cover.



- Notes:
1. The 0.72-in. width was the diameter of field, viewed through the eyepiece.
  2. Particle count was made by scanning in horizontal direction, with particles counted and recorded in each grid area.

Figure 6. Particle count grid pattern.

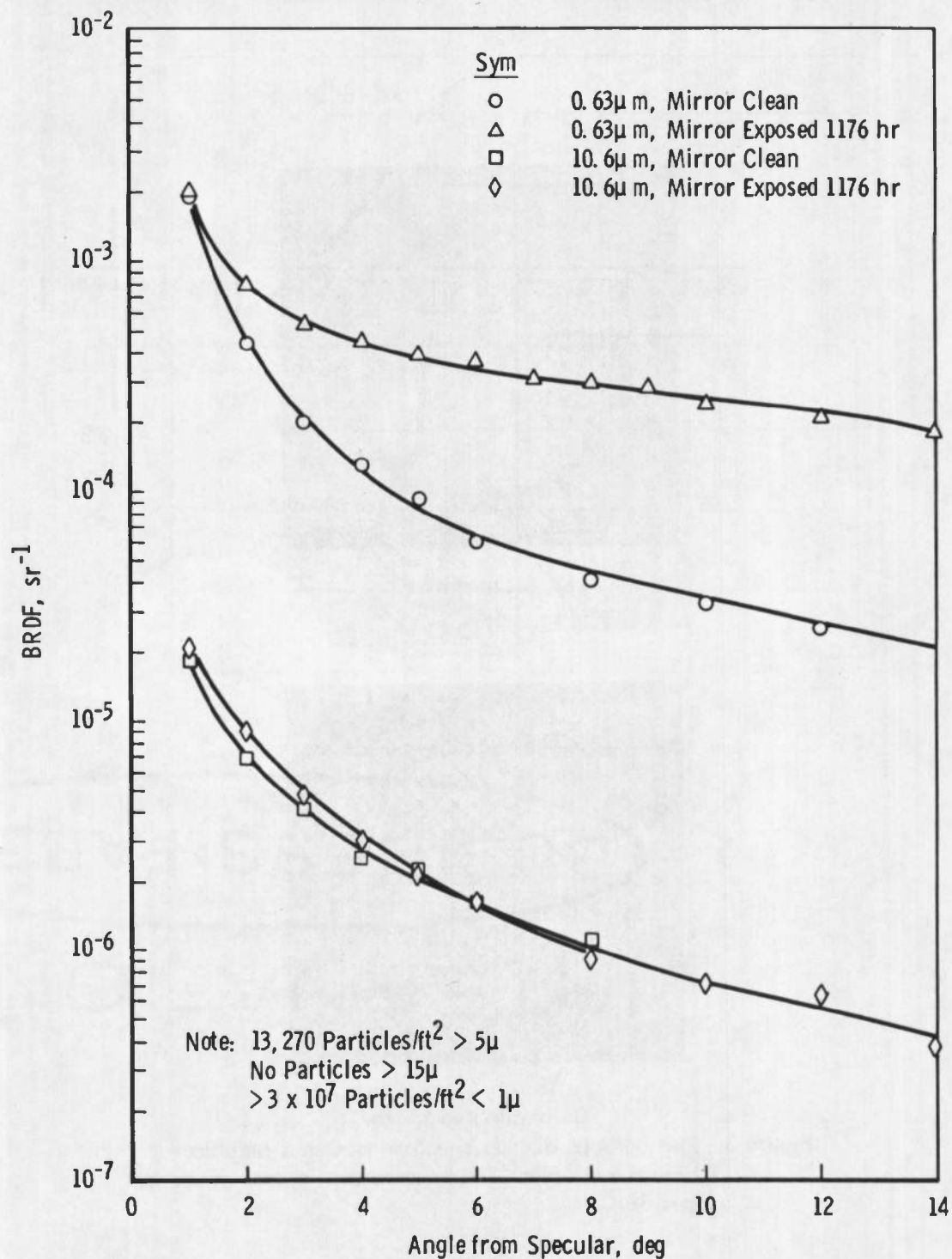
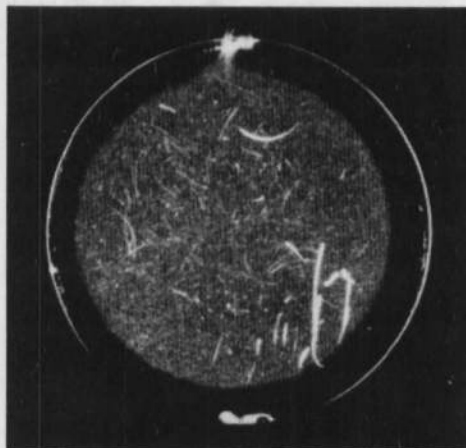
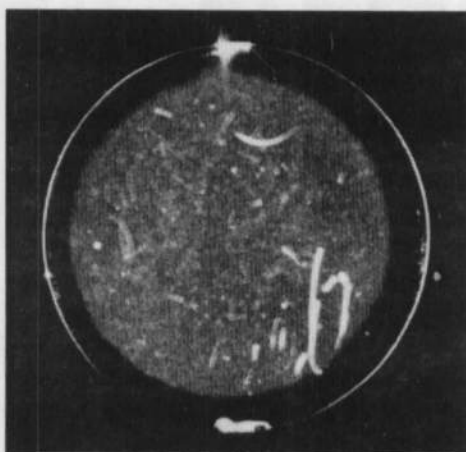


Figure 7. BRDF before and after 1176 hr exposure, mirror position vertical.

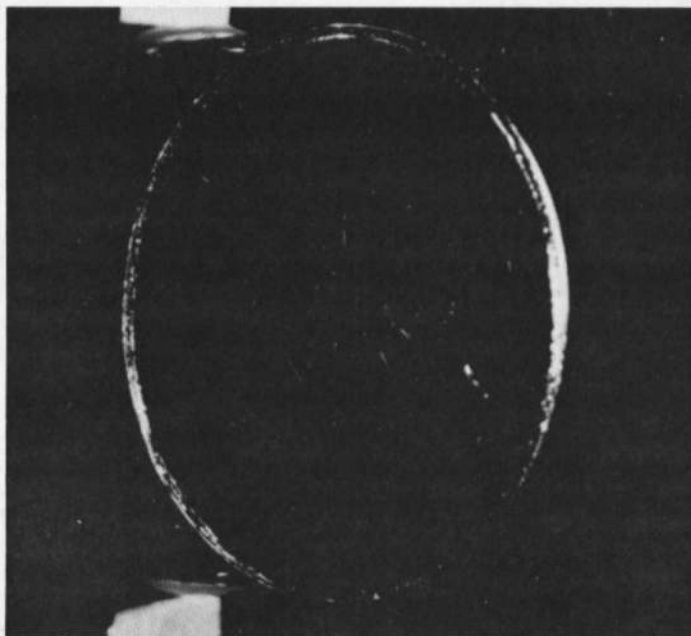


a. Clean mirror

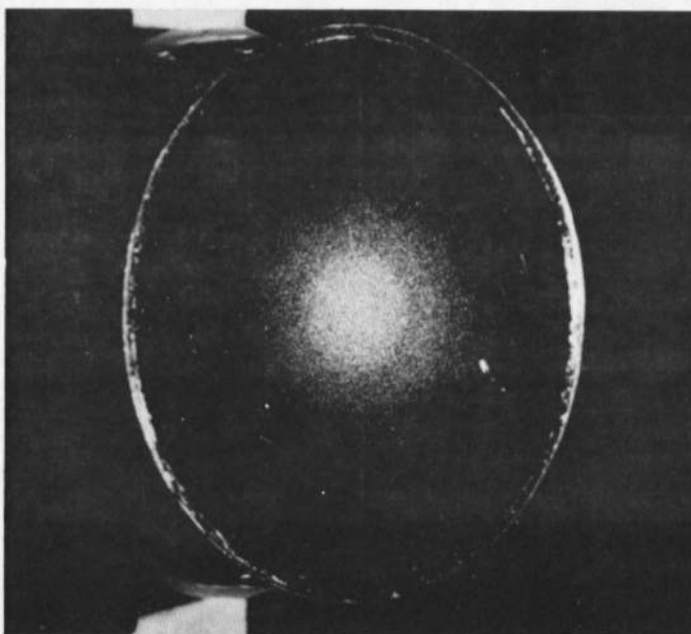


b. Contaminated mirror

**Figure 8. Photographs of near specular scattered radiation before and after 1176-hr exposure, mirror in vertical position.**



a. Clean mirror



b. Contaminated mirror

Figure 9. Photographs of scattered radiation at 10 deg from specular, before and after 1176-hr exposure, mirror in vertical position.

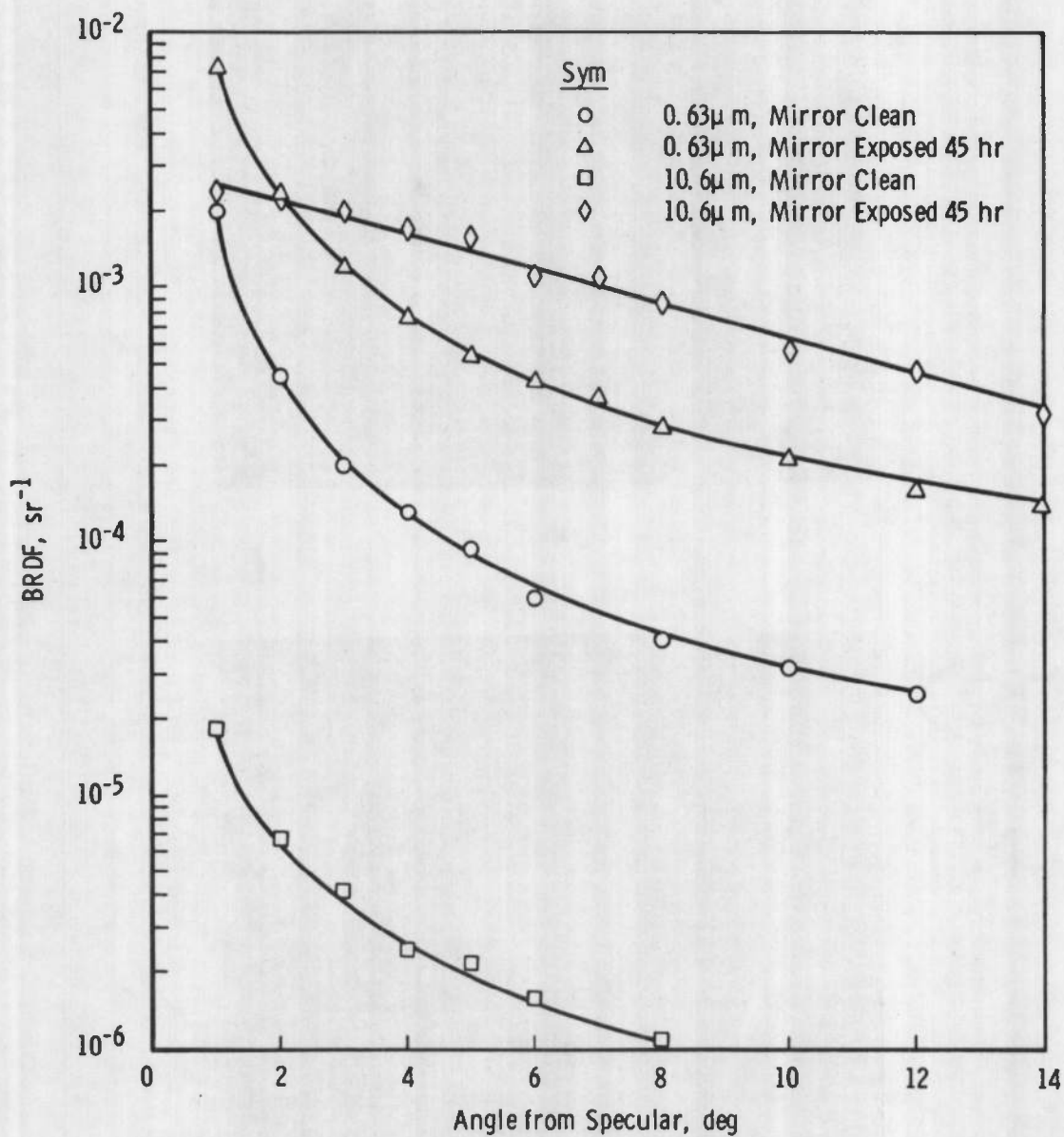
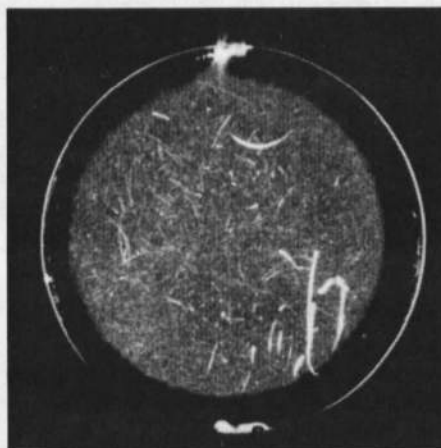
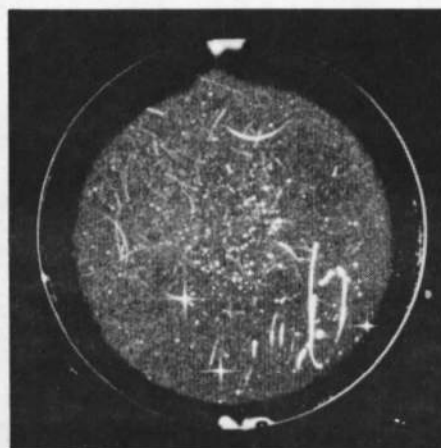


Figure 10. BRDF before and after 45-hr exposure, mirror position horizontal.



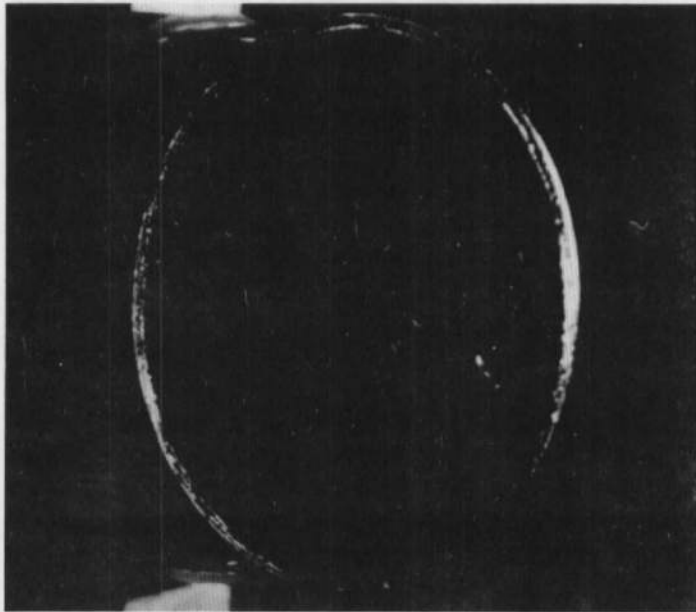


a. Clean mirror

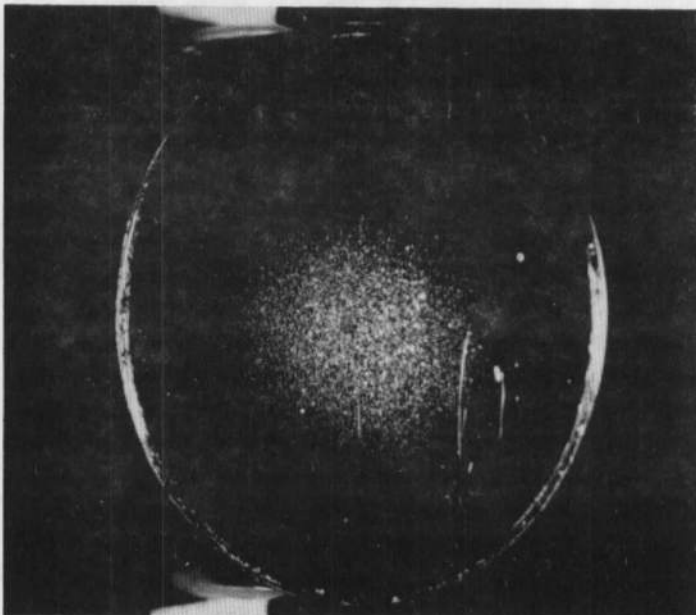


b. Contaminated mirror

**Figure 11.** Photographs of near specular scattered radiation before and after 45-hr exposure, mirror in horizontal position.



a. Clean mirror



b. Contaminated mirror

Figure 12. Photographs of scattered radiation at 10 deg from specular, before and after 45-hr exposure, mirror in horizontal position.



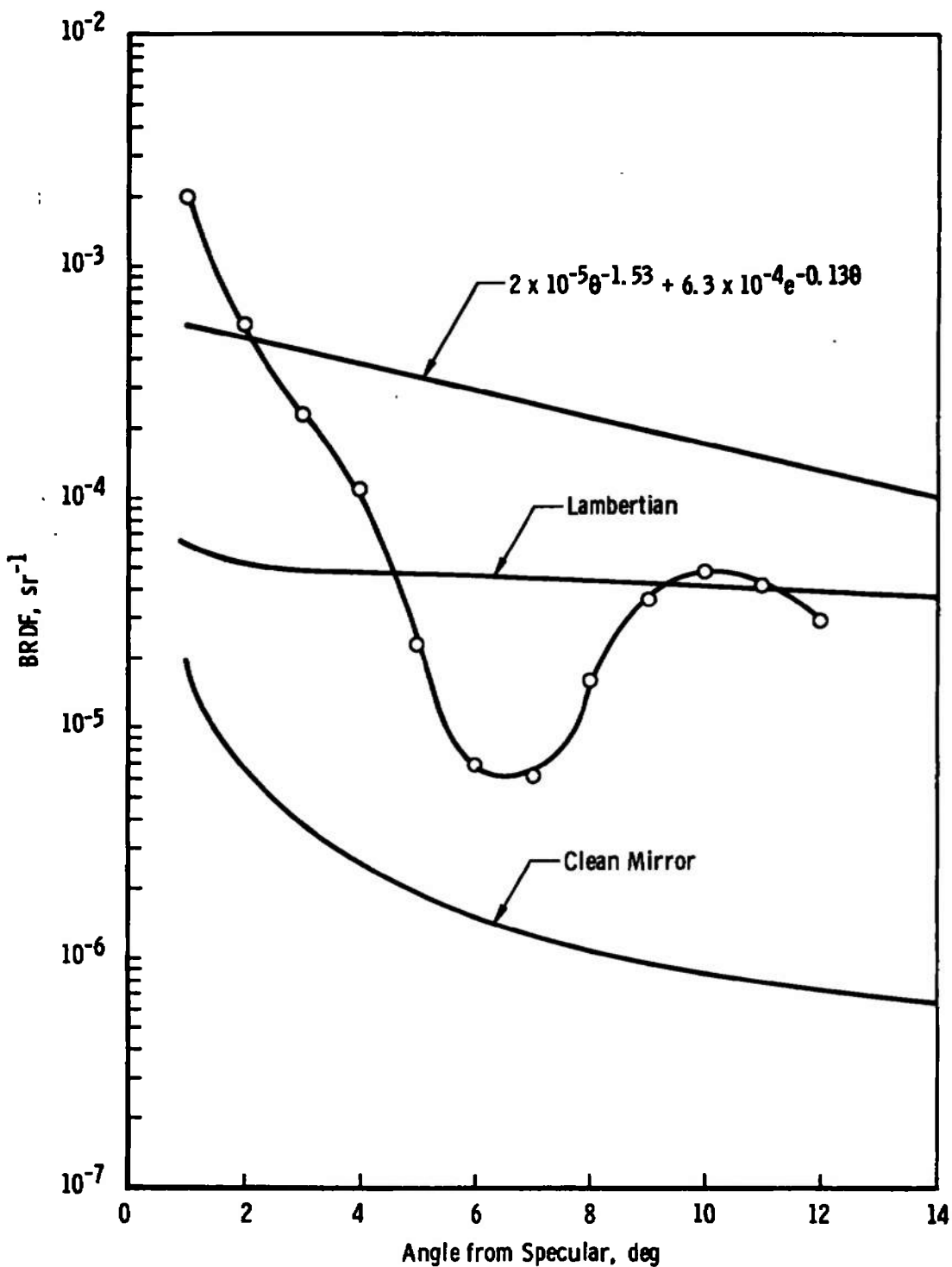


Figure 13. Mirror BRDF with one 750- by 30- $\mu\text{m}$  fiber on optical surface.

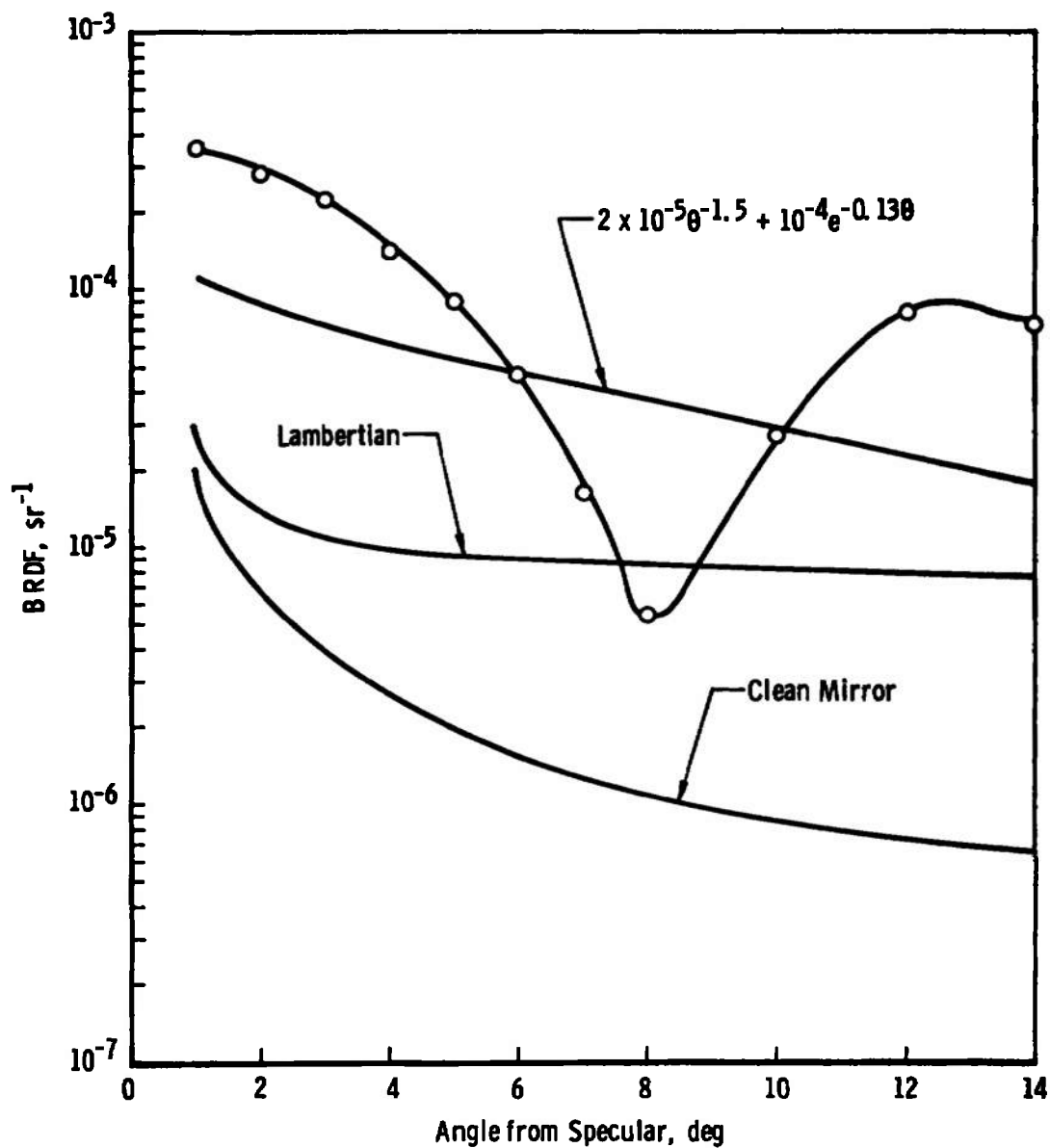


Figure 14. Mirror BRDF with one 90- by 35- $\mu\text{m}$  particle on optical surface.

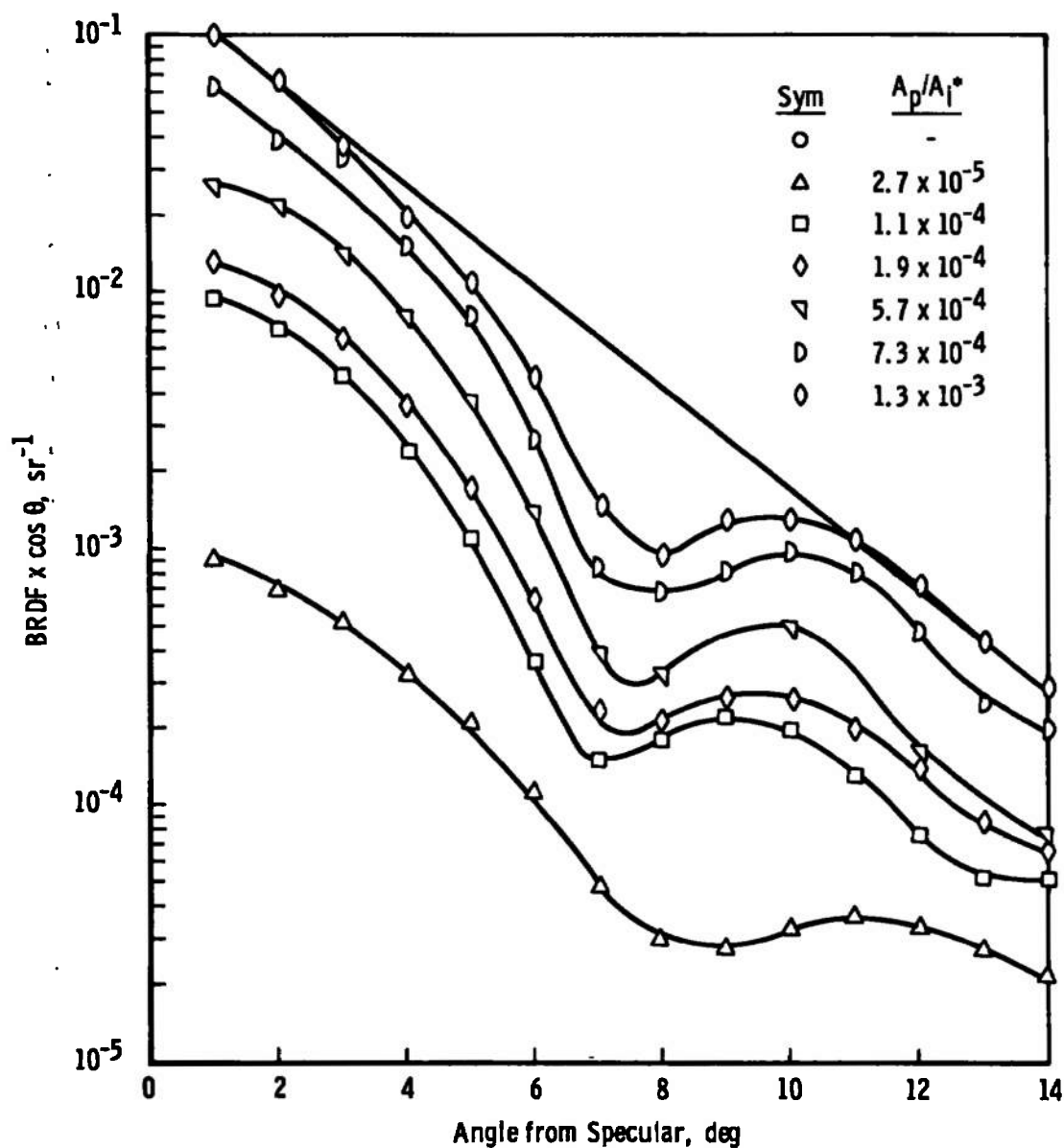


Figure 15. Mirror BRDF with glass bead (62- to 88-μm-diam) contaminant on optical surface.

**Table 1. Particle Count in Laser Laboratory Air**

Particle Size, $\mu\text{m}$	No. of Particles Greater than Stated Size/ $\text{ft}^3$
1.4	>100,000
3	1,600
5	500

Note: Measurements were made using a  
Model 245 Ryco Instruments  
particle counter.

**Table 2. Contamination Constants for Mirror Contaminated in Laser Laboratory**

Run No.	Mirror Position	Time Exposed, hr	No. of Particles in Size Range				$A_p/A_1$	$C_1$	$C_2$
			5 to 15 $\mu\text{m}$	15 to 30 $\mu\text{m}$	30 to 75 $\mu\text{m}$	>75 $\mu\text{m}$ L x W			
32	Vertical*	179	11	2	0	0	$8.0 \times 10^{-6}$	7.1	0.086
34	↓	247	9	↓	↓	↓	$7.4 \times 10^{-6}$	12.6	0.11
36		339	9	↓	↓	↓	$7.4 \times 10^{-6}$	5.5	0.094
38		413	8	↓	2	↓	$3.4 \times 10^{-5}$	2.2	0.093
72	Horizontal	2	14	4	1	460 x 25	$9.8 \times 10^{-5}$	7.4	0.2
73**	↓	2	15	4	1	0	$2.7 \times 10^{-5}$	4.3	0.16
74		4	36	8	4	↓	$8.2 \times 10^{-5}$	2.0	0.095
75		6	41	11	4	↓	$9.2 \times 10^{-5}$	1.7	0.095
76		10	168	33	6	↓	$2.0 \times 10^{-4}$	1.8	0.085
77		14	213	45	11	100 x 20	$3.3 \times 10^{-4}$	1.8	0.092
78		22	298	45	17	500 x 20 100 x 20 85 x 15	$5.0 \times 10^{-4}$	4.6	0.17
79**		22	298	45	17	100 x 20 85 x 15	$4.4 \times 10^{-4}$	4.3	0.18
80		29	412	68	19	100 x 20	$5.4 \times 10^{-4}$	4.3	0.17
81		45	405	75	29	100 x 20 100 x 35	$7.1 \times 10^{-4}$	3.9	0.16

\*Mirror cover was not used on these runs.

\*\*Blew off large particle from previous run.

**Table 3. Contamination Constants for Mirror Contaminated with Glass Beads**

Run No.	No. of Beads	$A_p/A_1$	$C_1$	$C_2$
46	21	$5.7 \times 10^{-4}$	100	0.46
48	49	$1.3 \times 10^{-3}$	123	0.45
49	27	$7.3 \times 10^{-4}$	137	0.44
50	7	$1.9 \times 10^{-4}$	137	0.44
51	4	$1.1 \times 10^{-4}$	164	0.48
55	3	$1.0 \times 10^{-4}$	190	0.72
56	10	$3.6 \times 10^{-4}$	77	0.39
57	21	$5.7 \times 10^{-4}$	140	0.41
58	6	$1.6 \times 10^{-4}$	63	0.35
59	2	$5.4 \times 10^{-5}$	148	0.34

Note:  $C_1$  average = 128

$C_2$  average = 0.45

## NOMENCLATURE

$A_i$	Area of mirror illuminated with radiation, $\text{cm}^2$
$A_p$	Summation of the projected areas of all particles on optical surface, $\text{cm}^2$
$C_1, C_2$	Contamination constants for empirical scatter equation
$P_i$	Incident power on mirror, watts
$P_m$	Scattered power from clean mirror, collected by telescope, watts
$P_p$	Scattered power from particles on mirror, collected by telescope, watts
$P_s$	Total scattered power from mirror surface, collected by telescope, watts
$R_D$	Reflectivity of diffuse reflector
$V_D$	Detector voltage with telescope viewing diffuse reflector, volts
$V_S$	Detector voltage from scattered radiation from mirror, volts
$\theta$	Telescope angle measured from the specularly reflected beam, deg
$\Omega$	Telescope acceptance solid angle, sr